

Energy Landscape of Charge Excitations in Boundary Region between Dimer-Mott and Charge Order State in Molecular Solids

Hidetoshi Fukuyama¹, Jun-ichiro Kishine², and Masao Ogata³

¹Department of Applied Physics, Faculty of Science, Tokyo University of Science, Shinjuku, Tokyo 162-8601, Japan

²Division of Natural and Environmental Sciences, The Open University of Japan, Chiba, 261-8586, Japan

³Department of Physics, University of Tokyo, Hongo 7-3-1, Bunkyo, Tokyo 113-0033, Japan

A possible theoretical scheme is proposed for the unified description of charge excitations with 10^{10} orders of magnitude difference in energy [from optical (\sim eV) down to dielectric anomalies (10KHz \sim 10^{-10} eV)] based on a simple and single model.

It has been established that the variety of ground states of strongly-correlated quarter-filled molecular solids can be systematically understood by noting dimer-Mott (DM) and charge ordering (CO) states as limiting cases controlled by the degree of dimerization.¹⁾ Recent experiments have disclosed remarkable and unexpected features of existence of charge excitations in such DM type insulators based on BEDT-TTF (ET) molecules: i.e., the existence of anomalous dielectric responses in κ -ET₂Cu₂(CN)₃ for frequency $\omega \sim 10$ KHz and in the temperature range $T < 50$ K,²⁾ while in β' -ET₂ICl₂ for $\omega \sim 100$ KHz and $T < 100$ K.³⁾ These experimental findings have disclosed the fact that charge fluctuations are possible even in apparent DM states and then these DM states are not in the limit of strong dimerization. These experimental findings have stimulated search for the exploration of new possibilities near the DM-CO boundary.

Theoretically, there are some studies^{2,4-6)} addressing to these intriguing properties of charge excitations near the DM-CO boundaries based on the tight-binding model in two-dimension with both dimerization and Coulomb interaction on site and inter site. We note, however, that the energy scale of the observed phenomena as dielectric anomalies is very small, e.g., $\hbar\omega \sim 10^{-10} - 10^{-9}$ eV for $\omega \sim 10$ K–100KHz, and then almost 10 orders of magnitude smaller than those in optical and infrared absorption with energy scale of the order of 1 eV, only the latter of which can be studied by the tight-binding model in a conventional way. In this paper we propose theoretically a possible scenario linking between such large energy differences based on a model Hamiltonian. Although the present theoretical studies are motivated by experiments on two-dimensional molecular solids, we adopt one-dimensional model because of mathematical transparency, and then comparison of the theoretical results with experimental findings is taken not truly quantitative but qualitative.

Our starting microscopic Hamiltonian is given as follows.

$$\mathcal{H} = - \sum_{j,\sigma} [t + (-1)^j t_d] (c_{j,\sigma}^\dagger c_{j+1,\sigma} + \text{h.c.}) + U \sum_j n_{j,\uparrow} n_{j,\downarrow} + V \sum_j n_j n_{j+1}, \quad (1)$$

where quarter-filling of the band is assumed, i.e., average electron number per site being 1/2. In the presence of finite dimerization, t_d , the original band is folded and becomes half-

filled in the reduced Brillouin zone, and hence t_d bridges between 1/4- and 1/2-filling smoothly. For theoretical studies of low energy excitations (compared with the Fermi energy ε_F) of one-dimensional systems such as the one represented by eq. (1), the phase Hamiltonian approach is very transparent and effective.^{7,8)} With finite t_d , eq. (1) can be transformed into the following⁹⁾ in terms of phase variables, $\theta(x)$, describing charge degrees of freedom where $[\theta(x), P(x')] = i\delta(x - x')$,

$$\mathcal{H} = \int dx \left[A_\rho (\partial_x \theta)^2 + C_\rho P(x)^2 - (g_{1/2} \sin 2\theta + g_{1/4} \cos 4\theta) / 2\pi^2 \alpha^2 \right], \quad (2)$$

where $A_\rho = (\hbar v_F / 4\pi) [1 + (U + 4V)a / \pi \hbar v_F]$, $C_\rho = \pi \hbar v_F$, $g_{1/2} = BUa$, $g_{1/4} = a^3 U^2 (4V - U) / 4\hbar^2 v_F^2$ with $\hbar v_F = 2ta \sin(k_F a) = 2ta \sin(\pi/4) = \sqrt{2}ta$ and $\alpha = a/\pi$,¹⁰⁾ are respectively Fermi velocity and cut-off parameter, where a is the lattice constant, and $B = 2t_d/t$. Equation (2) can further be rewritten as follows in terms of $\varphi = \theta - \pi/4$.

$$\mathcal{H} = \varepsilon_F \int dy \left[A (\nabla \varphi)^2 + P^2 + \mathcal{V}(\varphi) \right], \quad (3)$$

where

$$A = \frac{1}{4\pi^2} (1 + u + 4v), \quad (4)$$

with $y = x/a$, $u = U/\varepsilon_F$, $v = V/\varepsilon_F$, and $\varepsilon_F = \pi \hbar v_F / a$ where ε_F is the Fermi energy. The potential $\mathcal{V}(\varphi)$ is defined by

$$\mathcal{V}(\varphi) = -g_D \cos 2\varphi + g_C \cos 4\varphi, \quad (5)$$

where

$$g_D = \frac{g_{1/2}}{2a\varepsilon_F} = \frac{t_d}{t} u, \quad (6)$$

$$g_C = \frac{g_{1/4}}{2a\varepsilon_F} = \frac{\pi^2}{8} u^2 (4v - u). \quad (7)$$

In $\mathcal{V}(\varphi)$, eq. (5), $\varphi = 0$ corresponds to DM state, while $\varphi = -\pi/4$ or $\pi/4$ to CO states, respectively. It is seen that $\mathcal{V}(\varphi)$ takes minimum at $\varphi = 0$, pure dimer-Mott state, as far as $g_D > 4g_C$, while this state becomes unstable once $g_D < 4g_C$. Actually $\mathcal{V}(\varphi)$ around pure DM state ($\varphi \sim 0$) is given by

$$\mathcal{V}(\varphi) = (g_C - g_D) - \frac{K_2}{2} \varphi^2 + \frac{K_4}{4} \varphi^4 + \mathcal{O}(\varphi^6)$$

$$= (g_C - g_D) + \frac{K_4}{4} (\varphi^2 - \varphi_0^2)^2 - \frac{K_2^2}{4K_4} + \mathcal{O}(\varphi^6), \quad (8) \quad \text{i.e.,}$$

with $K_2 = 4(4g_C - g_D)$ and $K_4 = \frac{8}{3}(16g_C - g_D)$. In Fig. 1, $\mathcal{V}(\varphi)$ dependences are shown with choices of $g_D = 5$ and $g_C = 1$ (a), and $g_D = 3$ and $g_C = 1$ (b), where the DM state and the CO state are the ground state, respectively.

In the following, we assume $K_2 > 0$, in which case minima of $\mathcal{V}(\varphi)$ locate at $\varphi = \pm\varphi_0$ with $\varphi_0 = (K_2/K_4)^{1/2}$ [Fig. 1 (b)]. We will study the case where g_D is appreciably larger than g_C but not so large so that $g_D < 4g_C$ is satisfied, which will be the case when DM state compete with CO state. From now on, we use the fixed choice of parameters, $g_D = 3$ and $g_C = 1$.

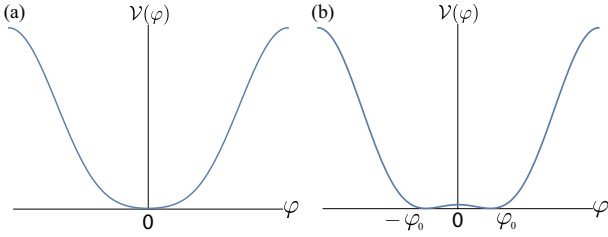


Fig. 1. Potential $\mathcal{V}(\varphi)$ with (a) $(g_D, g_C) = (5, 1)$ and (b) $(g_D, g_C) = (3, 1)$, where the DM and CO states are the ground states, respectively.

We will show that there exist four different characteristic energy scales, E_1, E_2, E_3 , and E_4 , of charge excitations in the case as shown in Fig. 1(b). Two energy scales (E_1, E_2) are in high energy quantum region, which are optical absorption across the Mott gap, E_1 , and uniform phase oscillation (phason) expected to be in infrared region, E_2 . Another two energy scales (E_3, E_4) are in low energy classical region, which are small uniform oscillation around either $\varphi = \varphi_0$ or $\varphi = -\varphi_0$, E_3 , and large amplitude spatial modulation bridging between them as described as a domain wall or a soliton to be associated with dielectric response, E_4 .¹³⁻¹⁵⁾

The largest energy scale of charge excitations, E_1 , governed by eq. (3) is the one due to $g_{1/2}$, which can be estimated by mapping eq. (3) (ignoring $g_{1/4}$) to the massive Thirring model of spinless fermions as described in.¹¹⁾ This corresponds to excitations across the Mott gap, and leads to

$$E_1 \sim \frac{2g_{1/2}}{\pi\alpha} = 2 \left(\frac{t_d}{t} \right) U = \varepsilon_F \left(2 \frac{t_d}{t} \right) u. \quad (9)$$

At lower energies, phasons start to be affected by the details of the restoring forces resulting from finite g_C in eq. (5). To assess this, $\mathcal{V}(\varphi)$ is treated as follows in a way similar to the self-consistent harmonic approximation,

$$\begin{aligned} \mathcal{V}(\varphi) &= -g_D \cos 2\varphi + g_C(2 \cos^2 2\varphi - 1) \\ &\sim -g_D \cos 2\varphi + 4g_C \langle \cos 2\varphi \rangle \cos 2\varphi \\ &= -\tilde{g}_D \cos 2\varphi = -\tilde{g}_D(1 - 2\varphi^2), \end{aligned} \quad (10)$$

where

$$\tilde{g}_D = g_D - 4g_C \langle \cos 2\varphi \rangle = g_D - 4g_C e^{-2\langle \varphi^2 \rangle}. \quad (11)$$

Here for \tilde{g}_D , frequency of uniform phason ω_0 around the pure DM state, $\varphi = 0$, governed by eq. (3) is given $\omega_0^2 = 8\tilde{g}_D \varepsilon_F^2 / \hbar^2$,

$$E_2 = \hbar\omega_0 = 2\sqrt{2\tilde{g}_D} \varepsilon_F. \quad (12)$$

The condition $0 < \tilde{g}_D$ together with $0 < K_2$ leads to

$$4g_C e^{-2\langle \varphi^2 \rangle} < g_D < 4g_C. \quad (13)$$

Eq. (13) will be easily satisfied since $\langle \varphi^2 \rangle$ is larger than the case of maximum restoring force \tilde{g}_D , i.e., g_D , for which

$$\exp[-2\langle \varphi^2 \rangle] < \exp\left(-\frac{1}{\sqrt{2g_D}}\right) = \exp\left(-\frac{1}{\sqrt{6}}\right) = 0.665, \quad (14)$$

for the present choice of $g_D = 3$.

At very low frequencies, we have to look more in detail of $\mathcal{V}(\varphi)$ which represents double potential minima for the case of $g_D < 4g_C$ indicating that pure dimer Mott state is unstable as seen in Fig. 1(b). This implies the intriguing fact that, if the quantum fluctuations are suppressed, pure dimer Mott states no longer exist, but have always small charge disproportionation with either $\varphi = \varphi_0$ or $\varphi = -\varphi_0$. Actually, in such low energy region the dynamics of phase variable will be treated classically since the quantum fluctuations intrinsic to purely one-dimensional systems as expressed by eq. (3) will no longer be the case because of the presence of three dimensionality of real systems.

The dynamical correlation in such situation with double potential minima in one-dimensional systems has been studied in the context of structural phase transition, which has clarified the existence of two different kinds of excitations, small amplitude oscillations around potential minima (φ_0 or $-\varphi_0$, here) on one hand, E_3 , and large amplitude spatial modulation bridging between the two minima described as a domain wall or a soliton, on the other hand. (In the structural phase transition the former is called as phonons, while the latter central modes¹²⁾). In the following we focus on the latter, E_4 .¹³⁻¹⁵⁾

For the present model defined by eqs. (3) and (8), the solution of an isolated soliton, φ_s , is given by

$$\varphi_s = \sqrt{\frac{K_2}{K_4}} \tanh\left[\frac{(\bar{y} - \bar{v}_d \bar{t})}{\sqrt{2}}\right], \quad (15)$$

where $\bar{y} = y/y_0$, $\bar{t} = (\varepsilon_F/\hbar) \sqrt{2K_2} t$, $\bar{v}_d = \hbar v_d / (y_0 a \varepsilon_F \sqrt{2K_2})$ with $y_0 = \sqrt{2A/K_2}$ and \bar{t}, \bar{v}_d are dimensionless time and velocity with real time t , and the drift velocity, v_d . The formation energy, E_{SF} , and kinetic energy, E_{SK} , associated with a single soliton are respectively given as follows,

$$E_{SF} = \frac{4}{3} \varepsilon_F \sqrt{A} \frac{K_2^{3/2}}{K_4}, \quad (16)$$

$$E_{SK} = \frac{2}{3} \varepsilon_F \sqrt{A} \frac{K_2^{3/2}}{K_4} \bar{v}_d^2 = \frac{1}{2} E_{SF} \bar{v}_d^2. \quad (17)$$

In terms of eq. (16), the number density of solitons per unit length n_s is given by

$$n_s = \frac{a}{\Delta} \sqrt{\frac{2\pi m_S}{\hbar^2 \beta}} e^{-\beta E_{SF}}. \quad (18)$$

Here we introduced the rest mass of a soliton

$$m_S = E_{SF} = \frac{4}{3} \varepsilon_F \sqrt{A} \frac{K_2^{3/2}}{K_4}. \quad (19)$$

Each soliton has a finite width $\Delta = 2\sqrt{A/K_2} a$. Because of this

width, we need to take account of the excluded volume effect which leads to a reduction factor a/Δ in eq. (18).

Regarding the anomalous dielectric properties, we first note that dielectric function $\varepsilon(\omega)$ is written as $\varepsilon(\omega) = 1 + 4\pi\sigma(\omega)/i\omega$ where $\sigma(\omega)$ is the dynamical conductivity computed by using the Kubo formula,

$$\begin{aligned}\varepsilon(\omega) &= 1 + \frac{4\pi\sigma(\omega)}{i\omega} \\ &= 1 + 2\pi\left(\frac{e}{\pi}\right)^2 L \mathcal{D}(0, 0; i\omega_n)|_{i\omega_n \rightarrow \omega + i\delta},\end{aligned}\quad (20)$$

The thermal Green function is defined by $\mathcal{D}(q, q'; i\omega_n) = \int_{-\beta}^{\beta} d\tau e^{i\omega_n\tau} \langle T_{\tau} \varphi_q(\tau) \varphi_{-q'} \rangle$, with $\omega_n = 2\pi n k_B T$, k_B and T being the Boltzmann constant and temperature, respectively.¹⁸⁾ The Fourier component φ_q is introduced by $\varphi(x) = L^{-1/2} \sum_q e^{iqx} \varphi_q$, and $\varphi_q(\tau) = e^{\tau H} \varphi_q e^{-\tau H}$ with $L = Na$ being the system size.

According to Ref.,¹⁶⁾ the dynamical correlation function, and then the frequency dependences of the dielectric function due to domain wall motions is given in the dilute limit of soliton (domain wall) density as follows, ($2t_s$ in Ref.¹⁶⁾ is written as τ_s here)

$$\varepsilon(\omega) \sim \varphi_0^2 \frac{\tau_s}{1 + \omega^2 \tau_s^2},\quad (21)$$

with τ_s being given by $\tau_s^{-1} = \int dv_d v_d n_S(v_d)$. The Maxwell distribution for the dilute soliton gas is given by

$$n_S(v) = \frac{m_S}{h} \frac{a}{\Delta} \exp\left[-\beta\left(\frac{1}{2}m_S v_d^2 + E_{SF}\right)\right],\quad (22)$$

which gives

$$\begin{aligned}E_4 &= \frac{h}{\tau_s} = \frac{1}{2\beta} \frac{a}{\Delta} e^{-\beta E_{SF}} = \frac{k_B T}{4} \sqrt{\frac{K_2}{A}} e^{-\beta E_{SF}} \\ &= \varepsilon_F \left(\frac{k_B T}{4\varepsilon_F}\right) \sqrt{\frac{K_2}{A}} \exp\left(-\frac{4}{3} \frac{\varepsilon_F}{k_B T} \sqrt{A} \frac{K_2^{3/2}}{K_4}\right).\end{aligned}\quad (23)$$

In Fig. 2, we show how the characteristic frequency scale, τ_s^{-1} , varies as a function of $k_B T/\varepsilon_F$, with our fixed choice of $g_D = 3$ and $g_C = 1$. It is clearly seen that τ_s^{-1} changes over 10 orders of magnitude over the temperature window around $T \sim 100\text{K}$ and the range of KHz is easily obtained.

Experimentally, however, the maximum indicate much weaker ω dependences²⁾ suggesting an interesting fact that solitons may not be moving freely and/or independently, due to mutual interactions between solitons¹⁷⁾ as described by the finite dispersions of the phason mode of soliton lattice or due to impurity pinning.¹⁸⁾ These will be subjects of further studies.

In summary we have demonstrated that there are four different energy scales in charge excitations in the Hamiltonian eq. (3), as schematically shown in Fig. 3. Here we point out that various effects associated with impurity or three-dimensionality may be manifested at energies below E_2 , which have not been focused on explicitly in the present study.

The present demonstrations will shed light on the possible microscopic understanding of experimental observations^{2,3)} of dielectric anomalies seen in the range of 10 KHz based on the familiar microscopic model Hamiltonian for electrons in solids describing the competitions between dimer-Mott and

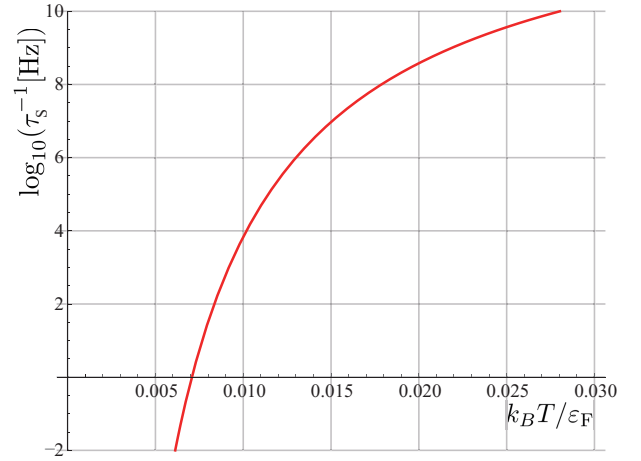


Fig. 2. Characteristic frequency of dielectric responses due to the central modes of domain walls (solitons), as a function of $k_B T/\varepsilon_F$, with our fixed choice of parameters, $g_D = 3$, $g_C = 1$, and $A = 0.1$.

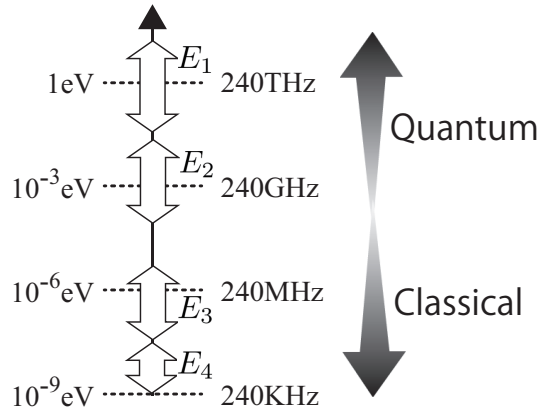


Fig. 3. Four different energy scales in charge excitations demonstrated in this letter. E_1 and E_2 are in high energy quantum region, while E_3 and E_4 are in low energy classical region.

charge ordering which are typical states in the presence of strong correlations in quarter-filled bands. It is to be noted that interesting phenomena observed in specific heat^{19,20)} and infrared optical measurements²¹⁾ are in different energy region from the present studies, though these will be mutually interrelated.

Finally, we give brief comments on the relevance of the present scheme to experimentally observed KHz dynamics in a mono-axial chiral helimagnet^{22,23)} near the boundary of magnetic phase transitions.²⁴⁾ This will be studied in detail elsewhere.

Acknowledgment Special thanks are due to T. Sasaki for very informative discussions in various stages. H.F. thanks H. Kishida, H. Seo and H. Yoshioka for discussions in early stage of the work. We thank M. Mito and A. S. Ovchinnikov for fruitful discussions. This work was supported by a Grant-in-Aid for Scientific Research (A) (No. 15H02108), (B) (No. 17H02923) and (S) (No. 25220803) from the MEXT of the Japanese Government, and the JSPS Core-to-Core Program, A. Advanced Research Networks.

- 1) H. Seo, C. Hotta and H. Fukuyama, *Chemical Review* **104** (2004) 5005.
- 2) M. Abdel-Jawad, I. Terasaki, T. Sasaki, N. Yoneyama, N. Kobayashi, Y. Uesu, and C. Hotta, *Phys. Rev. B* **82** (2010) 125119.
- 3) S. Iguchi, S. Sasaki, N. Yoneyama, H. Taniguchi, T. Nishizaki, and T. Sasaki, *Phys. Rev. B* **87** (2013) 075107.
- 4) M. Naka, and S. Ishihara, *J. Phys. Soc. Jpn.* **79** (2010) 063707.
- 5) C. Hotta, *Phys. Rev. B* **82** (2010) 241104(R).
- 6) C. Hotta, *Crystals* **2** (2012) 1155.
- 7) Y. Suzumura, *Prog. Theor. Phys.* **61** (1979) 1.
- 8) H. Fukuyama and H. Takayama, *Electronic Properties of Inorganic Quasi One Dimensional Compounds*, ed. P. Monceau (D. Reidel Publishing Co., 1985) p.41-104.
- 9) M. Tsuchiizu, H. Yoshioka, and Y. Suzumura, *J. Phys. Soc. Jpn.* **70** (2001) 1460.
- 10) T. Nakano and H. Fukuyama, *J. Phys. Soc. Jpn.* **49** (1980) 1679.
- 11) M. Mori and H. Fukuyama, *J. Phys. Soc. Jpn.* **65** (1996) 3604.
- 12) J.F.Scott, *Rev. Mod. Phys.* **46** (1974) 83.
- 13) Domains have actually been observed near the boundary between Mott insulating and metallic states.^{14,15} Spatial contrast will not be so strong in the present case since $|\varphi_0|$ can be very small.
- 14) T. Sasaki, N. Yoneyama, N. Kobayashi, Y. Ikemoto and H. Kimura, *Phys. Rev. Lett.* **92**, (2004) 227001.
- 15) T. Sasaki, N. Yoneyama, A. Suzuki, N. Kobayashi, Y. Ikemoto and H. Kimura, *J. Phys. Soc. Jpn.* **74** (2005) 2351.
- 16) J. A. Krumhansl and J. R. Schrieffer, *Phys. Rev. B* **11** (1975) 3535.
- 17) J. Kishine and A. S. Ovchinnikov, arXiv:1609.03009v1.
- 18) H. Fukuyama, *J. Phys. Soc. Jpn.* **41** (1976) 1137.
- 19) K. Biljaković, D. Starešinić, J.C. Lasjaunias, G. Remenyi, R. Mélin, P. Monceau, and S. Sahling, *Physica B* **407**, 1741 (2012).
- 20) K. Biljaković, D. Starešinić, D. Dominko and J.C. Lasjaunias, *Physica B* **404** (2009) 456.
- 21) M. Dressel, P. Lazić, A. Pustogow, E. Zhukova, B. Gorshunov, J. A. Schlueter, O. Milat, B. Gumhalter, and S. Tomić, *Phys. Rev. B* **93** (2016) 081201.
- 22) J. Kishine and A. S. Ovchinnikov, "Theory of Monoaxial Chiral Helimagnet," in *Solid State Physics* **66** (Elsevier Inc., 2015) 1st ed., pp. 1-30.
- 23) Y. Togawa, Y. Kousaka, K. Inoue and J. Kishine, *J. Phys. Soc. Jpn.* **85** (2016) 112001.
- 24) K. Tsuruta, M. Mito, H. Deguchi, J. Kishine, Y. Kousaka, J. Akimitsu, and K. Inoue, *Phys. Rev. B* **93** (2016) 104402.